$Na_{12}Ge_{17}$: A Compound with the Zintl Anions $[Ge_4]^{4-}$ and $[Ge_9]^{4-}$ – Synthesis, Crystal Structure, and Raman Spectrum

W. Carrillo-Cabrera*[,a], **R. Cardoso Gil**[a], **M. Somer**[b], **Ö. Persil**[b], **and H. G. von Schnering**[c]

[a] Dresden, Max-Planck-Institut für Chemische Physik fester Stoffe
[b] Sariyer-Istanbul/Turkey, Chemistry Department, Koç University
[c] Stuttgart, Max-Planck-Institut für Festkörperforschung

Received December 12th, 2002.

Professor Wolfgang Brockner zum 65. Geburtstag gewidmet

Abstract. $Na_{12}Ge_{17}$ is prepared from the elements at 1025 K in sealed niobium ampoules. The crystal structure reinvestigation reveals a doubling of the unit cell (space group: $P2_1/c$; a = 22.117(3) Å, b = 12.803(3) Å, c = 41.557(6) Å, β = 91.31(2)°, Z = 16; Pearson code: *mP*464), furthermore, weak superstructure reflections indicate an even larger *C*-centred monoclinic cell. The characteristic structural units are the isolated cluster anions $[Ge_9]^{4-}$ and $[Ge_4]^{4-}$ in ratio 1:2, respectively. The crystal structure represents a hierarchical cluster replacement structure of the hexagonal Laves phase $MgZn_2$ in which the Mg and Zn atoms are replaced by the Ge_9 and Ge_4 units, respectively. The Raman spectrum of $Na_{12}Ge_{17}$ exhibits the characteristic breathing modes of the constituent cluster anions at $\nu = 274\ cm^{-1}$ ($[Ge_9]^{4-}$) and $\nu = 222\ cm^{-1}$ ($[Ge_4]^{4-}$) which may be used for identification of these clusters in solid phases and in solutions. Raman spectra further prove that $Na_{12}Ge_{17}$ is partial soluble both in ethylenediamine and liquid ammonia. The solution and the solid extract contain solely $[Ge_9]^{4-}$. The remaining insoluble residue is Na_4Ge_4. By heating the solvate $Na_4Ge_9(NH_3)_n$ releases NH_3 and decomposes irreversibly at 742 K, yielding $Na_{12}Ge_{17}$ and Ge.

Keywords: Zintl anions; Germanium; Raman spectroscopy

$Na_{12}Ge_{17}$: Eine Verbindung mit den Zintl-Anionen $[Ge_4]^{4-}$ und $[Ge_9]^{4-}$: Darstellung, Kristallstruktur und Ramanspektrum

Inhaltsübersicht. $Na_{12}Ge_{17}$ wurde durch direkte Umsetzung der Elemente in verschweißten Nb-Ampullen bei 1025 K synthetisiert. Die erneute Bestimmung der Kristallstruktur ergab eine Verdopplung der Elementarzelle (Raumgruppe $P2_1/c$, a = 22.117(3) Å, b = 12.803(3) Å, c = 41.557(6) Å, β = 91.31(2)°, Z = 16; Pearsonsymbol: *mP*464), jedoch zeigen schwache Überstrukturreflexe eine noch größere *C*-zentrierte monokline Elementarzelle an. Die charakteristischen Strukturelemente sind isolierte Clusteranionen $[Ge_9]^{4-}$ und $[Ge_4]^{4-}$ im Molverhältnis 1:2. Die Kristallstruktur ist eine hierarchische Cluster-Ersetzungs-Struktur der hexagonalen Laves-Phase $MgZn_2$, in welcher die Mg- bzw. Zn-Atome durch die Cluster $[Ge_9]^{4-}$ bzw. $[Ge_4]^{4-}$ ersetzt sind. Das Ramanspektrum von $Na_{12}Ge_{17}$ zeigt die charakteristischen Pulsationsfrequenzen der Clusteranionen bei $\nu = 274\ cm^{-1}$ ($[Ge_9]^{4-}$) und $\nu = 222\ cm^{-1}$ ($[Ge_4]^{4-}$), die also zur Identifizierung dieser Einheiten in fester Phasen und Lösungen verwendet werden können. Ferner beweisen die Ramanspektren, dass $Na_{12}Ge_{17}$ sowohl in Ethylendiamin als auch in flüssigem Ammoniak partiell löslich ist. Die Lösung und das Feststoffextrakt enthalten ausschließlich $[Ge_9]^{4-}$, während der unlösliche Rückstand nur aus Na_4Ge_4 besteht. Bei Erhitzen von $Na_4Ge_9(NH_3)_n$ wird NH_3 abgespalten und die Verbindung zersetzt sich bei 742 K zu $Na_{12}Ge_{17}$ und Ge.

1 Introduction

The binary system Na−Ge has been investigated quite extensively by thermal analytical and crystallographic methods already in the early 1950's [1, 2]. The results of these studies indicated the existence of congruent melting NaGe, later recognised as Na_4Ge_4 by a X-ray single crystal diffraction study [3]. The phase diagram of the binary Na−Ge [4] shows beside NaGe (Na_4Ge_4) two other congruent melting phases namely Na_3Ge and '$NaGe_4$', the latter being identified as Ge [5] while Na_3Ge is structurally not characterised yet.

1970 *Diehl* and *Kummer* [6, 7] synthesised the *en* (*en* = ethlenediamine) solvate $[Na(en)_7]Ge_9$ using the alloy $NaGe_{2.25}$ as a precursor. In 1984, *Llanos* obtained a '$NaGe_{1.3}$' phase by thermal decomposition of Na_4Ge_4 [8]. Later [5], this phase was identified as $Na_{12}Ge_{17}$ with the unit cell a = 20.834 Å, b = 12.817 Å, c = 22.191 Å, β = 91.43°. However, the structure determination and refinement were not satisfactory, due to the very poor quality of the crystal. In the following, we report the results of the reinvestigation of $Na_{12}Ge_{17}$ by X-ray single crystal diffraction and Raman spectroscopy.

2 Crystal Structure Determination

The best single crystal of $Na_{12}Ge_{17}$ was chosen for the X-ray diffraction measurement (unit cell **I:** a = 22.117(3) Å, b = 12.803(3) Å, c = 41.557(6) Å, β = 91.31(2)°). Consider-

---

* Dr. W. Carrillo-Cabrera
Max-Planck-Institut für Chemische Physik fester Stoffe
Nöthnitzer Straße 40
D-01187 Dresden
Email: carrillo@mpg.cpfs.de

Table 1 Selected crystallographic data (293 K).

Compound; molar mass	$Na_{12}Ge_{17}$; 1510.25 amu
Crystal	dark grey fragment (0.14×0.13×0.11 mm)
Space group; Pearson code	$P2_1/c$ (No. 12); *mP*464
Unit cell; formula units	a = 22.117(3) Å, b = 12.803(3) Å, c = 41.557(6) Å, β = 91.31(2)°, V = 11764(4) $Å^3$; Z = 16
d_{calc}	3.411 $g \cdot cm^{-3}$
Data collection	STOE-IPDS, $\lambda(AgK_\alpha)$ = 0.56087 Å, 450 exposures, $\Delta\phi$ = 0.4°; 2.1° $< 2\theta <$ 29.2°
Data correction	Numerical absorption correction [9, 10]. μ = 90.5 cm^{-1}; transmission: 0.331−0.419
Structure solution	Direct methods, SHELXLS-97 [11] Refinement on F^2, SHELXL-97 [12] (513 variable parameters)
N(hkl): measured; unique	31115; 8953
$N'(hkl)$ with $I > 3 \cdot \sigma(I)$; $I > 2 \cdot \sigma(I)$	3064; 4119
$R_{gt}(F)$, $wR_{gt}(F^2)$	0.095, 0.144 ($I > 3 \cdot \sigma(I)$) 0.118, 0.153 ($I > 2 \cdot \sigma(I)$)
$wR_{all}(F^2)$	0.167

ation of all measured reflections revealed a larger *C*-centred monoclinic unit cell **II** (a' = 44.23 Å, b' = 25.60 Å, c' = 46.63 Å, β' = 117.0°; the relation between unit cell **II** and unit cell **I** is: $\vec{a}' = 2\vec{a}$, $\vec{b}' = -2\vec{b}$, $\vec{c}' = -\vec{a}-\vec{c}$). But, the intensity data were very poor (only 14 % of the measured reflections had $I > 2 \cdot \sigma(I)$) and the structure solution with direct methods failed. In detail, the reflections which were necessary to chose the larger unit cell **II** instead of a smaller one were comparatively weak ($I < 8\sigma(I)$, representing 19 % of the observed reflections). Neglecting these reflections, the data could be indexed for a smaller primitive monoclinic unit cell (**I**) and the space group was determined to be $P2_1/c$ (No. 14).

Direct methods ($|E| > 1.1$) were used to solve the crystal structure. The E map of the best solution yielded the location of all the germanium atoms and most of the sodium atoms. The positions of the remaining Na atoms were revealed through difference Fourier syntheses (calculations were performed using the programs listed in Table 1, see also section 4). The refinement of the structure converged rapidly and a conventional R_{gt} value of 0.142 (for $I > 2 \cdot \sigma(I)$) was obtained for a model with isotropic displacement parameters (the number of observed reflections is not large enough for a reliable refinement with anisotropic displacement parameters). The Fourier syntheses and the large displacement parameters for several Ge positions indicated splitting of each one of those sites into two sites, both with SOF = 0.50 (a similar solution model with split positions resulted in the non-centrosymmetric space group $P2_1$). The final refinement for the split-model converged to a R_{gt} value of 0.118 for $I > 2 \cdot \sigma(I)$ (a R_{gt} value of 0.095 was obtained for $I > 3 \cdot \sigma(I)$).

The crystallographic data, the positional and isotropic displacement parameters, and the important distances d(Ge−Ge) are listed in Table 1, Table 2 and Table 3, respectively. Further details are available from the Fachinformationszentrum Karlsruhe, D-76344 Eggenstein-Leopoldshafen (Germany), on quoting the depository number CSD-412932, the name of the author(s), and the citation paper.

3 Results and Discussion

3.1 Crystal Structure

As mentioned in section 2, the present X-ray reinvestigation on $Na_{12}Ge_{17}$ reveals that the unit cell (**I**) is two times larger than the one previously reported [5]. Furthermore, weak reflections ($I < 8\sigma(I)$) indicate an even larger *C*-centred monoclinic unit cell **II** (a' = 44.23 Å, b' = 25.60 Å, c' = 46.63 Å, β' = 117.0°). This indicates a further orientational ordering of those Ge_9 clusters, which show some disordering in the unit cell **I,** as presented below.

The crystal structure of $Na_{12}Ge_{17}$ (non-split average model) contains four and eight crystallographically independent $[Ge_9]^{4-}$ and $[Ge_4]^{4-}$ cluster ions, respectively.

Regarding only the packing of the Zintl anions $[Ge_9]^{4-}$ and $[Ge_4]^{4-}$, the structure can be described as a hierarchical cluster replacement derivative [13] of the hexagonal $MgZn_2$ structure (*basic* structure or hierarchy *initiator*). As shown in Fig. 1, the Ge_9 and Ge_4 units substitute the Mg and Zn atoms, respectively, and the Na atoms occupy 12 of the 17 tetrahedral holes of the pseudo-hexagonal packing (most of the Na atoms are off-centre and several of them are significantly relaxed towards the empty □ sites). The formula can be written as: $Na_{12}Ge_{17} = (Na^+)_{12}\square_5[Ge_9^{4-}][Ge_4^{4-}]_2 \;\widehat{=}\; \square_{17}[Mg][Zn]_2$.

In this description, the quasi-hexagonal axis of $Na_{12}Ge_{17}$, $c_{h'} = c = 2 \cdot c(MgZn_2)$, is two times larger than that of an equivalent $MgZn_2$ arrangement. Apart of the effect of the unfilled □ tetrahedral holes, the deformation of the formally hexagonal unit cell to a monoclinic one is mainly a result of the site colouring due to the different orientations of the 'non-spherical' Ge_9 clusters for a better packing in the crystal. Further cluster site colouring of this kind might causes the additional enlargement of the unit cell. The doubling of $c_{h'}$ also results from this colouring and not from a change in the layer stacking sequence as in $MgNi_2$.

Because of the hierarchical relationship of $Na_{12}Ge_{17}$ with $MgZn_2$, the characteristic topological features are unchanged. Thus, as illustrated in Fig. 1b, 2D 3.6.3.6 Kagomé nets parallel to the (001) plane are formed by connecting the centres of the Ge_4 tetrahedral anions. By further connecting the nodes of these Kagomé nets with intermediate sites along the *c*-axis, a 3D framework with tetrahedral and truncated tetrahedral holes is formed. One tetrahedron of Ge_4 tetrahedra (a *supertetrahedron*) centred by a Na^+ cation is shown in Fig. 2b. Also, one truncated tetrahedron of Ge_4 tetrahedra (a *trucated supertetrahedron*) centred by a $[Ge_9]^{4-}$ anion is illustrated in Fig. 2a. Thus, each Ge_9 cluster is coordinated by 12 Ge_4 units and 4 Ge_9 units (the latter not shown in Fig. 2a), forming a CN-16 Frank-Kasper or Friauf *superpolyhedron.*

To easy the recognition of the atoms belonging to a Ge_n cluster, they were labelled as Ge(*i*Y), where i = 1−4 (for

Table 2 Atomic coordinates and isotropic displacement parameters (in Å^2 × 10^3) for $Na_{12}Ge_{17}$. All atoms at 4*e* sites. Ge positions with 50 % occupancy (SOF = 0.5) are indicated by *. Standard deviations are given in parentheses.

Atom	*x*	*y*	*z*	U_{iso}	Atom	*x*	*y*	*z*	U_{iso}
Ge(1A)	0.4420(3)	0.7930(5)	0.0928(2)	30(2)	Ge(1J′)*	0.502(1)	0.134(1)	0.5265(5)	35
Ge(2A)	0.5502(4)	0.1243(6)	0.3729(2)	33(2)	Ge(2J)	0.4276(4)	0.2131(6)	0.4831(2)	38(2)
Ge(3A)	0.3545(3)	0.7367(6)	0.1305(2)	34(2)	Ge(3J)*	0.4102(8)	0.075(1)	0.5347(4)	26(3)
Ge(4A)	0.4532(4)	0.8060(6)	0.1540(2)	38(2)	Ge(3J′)*	0.3930(8)	0.083(1)	0.5446(4)	26
Ge(1B)	0.1843(4)	0.0382(6)	0.944(2)	33(2)	Ge(4J)	0.4604(4)	0.2219(6)	0.5781(2)	38(2)
Ge(2B)	0.2210(4)	0.9596(6)	0.1477(2)	32(2)	Ge(5J)*	0.486(1)	0.361(2)	0.5295(5)	35(4)
Ge(3B)	0.1277(4)	0.0789(6)	0.1455(2)	33(2)	Ge(5J′)*	0.489(1)	0.339(2)	0.5213(5)	35
Ge(4B)	0.1244(4)	0.8973(6)	0.1202(2)	44(2)	Ge(6J)	0.3755(4)	0.3740(6)	0.5045(2)	38(2)
Ge(1C)	0.9869(3)	0.2338(6)	0.1139(2)	33(2)	Ge(7J)	0.3229(4)	0.1941(6)	0.5092(2)	40(2)
Ge(2C)	0.1155(3)	0.8270(5)	0.3959(2)	30(2)	Ge(8J)*	0.3439(9)	0.194(1)	0.5707(4)	35(3)
Ge(3C)	0.1117(4)	0.6358(6)	0.3764(2)	38(2)	Ge(8J′)*	0.3410(9)	0.241(1)	0.5709(4)	35
Ge(4C)	0.0769(4)	0.7835(6)	0.3385(2)	41(2)	Ge(9J)*	0.397(1)	0.379(2)	0.5663(6)	38(3)
Ge(1D)	0.3004(3)	0.7076(6)	0.2298(2)	36(2)	Ge(9J′)*	0.412(1)	0.395(2)	0.5638(6)	38
Ge(2D)	0.2351(3)	0.8721(6)	0.2346(2)	33(2)	Ge(1K)	0.1744(4)	0.3547(6)	0.4640(2)	53(3)
Ge(3D)	0.2596(3)	0.7620(5)	0.2842(2)	31(2)	Ge(2K)	0.0864(4)	0.3228(7)	0.4224(2)	56(3)
Ge(4D)	0.1878(4)	0.6867(6)	0.2402(2)	38(2)	Ge(3K)*	0.159(1)	0.168(2)	0.4480(4)	39(4)
Ge(1E)	0.3841(3)	0.4572(6)	0.3474(2)	29(2)	Ge(3K′)*	0.165(1)	0.148(2)	0.4578(4)	39
Ge(2E)	0.2821(4)	0.5435(6)	0.3575(2)	32(2)	Ge(4K)	0.1435(4)	0.2389(6)	0.5108(2)	42(2)
Ge(3E)	0.3219(3)	0.3988(5)	0.3952(2)	29(2)	Ge(5K)*	0.0719(8)	0.405(1)	0.4873(4)	39(4)
Ge(4E)	0.3711(4)	0.5763(5)	0.3960(2)	32(2)	Ge(5K′)*	0.0670(9)	0.419(1)	0.4729(4)	39
Ge(1F)	0.3543(4)	0.9149(6)	0.3527(2)	37(2)	Ge(6K)*	0.992(1)	0.303(1)	0.4557(5)	46(4)
Ge(2F)	0.3112(4)	0.0967(6)	0.3601(2)	34(2)	Ge(6K′)*	0.991(1)	0.265(1)	0.4555(5)	46
Ge(3F)	0.3916(4)	0.0280(6)	0.4003(2)	31(2)	Ge(7K)*	0.0486(4)	0.147(2)	0.4280(5)	39(3)
Ge(4F)	0.2852(3)	0.9522(5)	0.3996(2)	27(2)	Ge(7K′)*	0.0643(4)	0.123(2)	0.4295(5)	39
Ge(1G)	0.3039(3)	0.7462(6)	0.4777(2)	35(2)	Ge(8K)*	0.084(1)	0.084(2)	0.4873(6)	47(4)
Ge(2G)	0.2389(4)	0.8356(5)	0.5182(2)	34(2)	Ge(8K′)*	0.065(1)	0.098(2)	0.4887(6)	47
Ge(3G)	0.1940(4)	0.6870(6)	0.4836(2)	45(2)	Ge(9K)*	0.0247(8)	0.238(1)	0.5111(4)	31(3)
Ge(4G)	0.2723(4)	0.6444(6)	0.5269(2)	34(2)	Ge(9K′)*	0.0377(8)	0.282(1)	0.5152(4)	31
Ge(1H)	0.1931(4)	0.5851(6)	0.1074(2)	36(2)	Ge(1L)*	0.1752(9)	0.377(1)	0.2816(5)	48(4)
Ge(2H)	0.1965(4)	0.3993(6)	0.1274(2)	34(2)	Ge(1L′)*	0.1871(9)	0.337(1)	0.2753(4)	48
Ge(3H)	0.1038(3)	0.4668(6)	0.0970(2)	27(2)	Ge(2L)*	0.0698(9)	0.422(2)	0.2897(4)	48(4)
Ge(4H)	0.1273(4)	0.5327(6)	0.1543(2)	35(2)	Ge(2L′)*	0.0844(9)	0.428(2)	0.2776(5)	48
Ge(1I)	0.6155(4)	0.6340(6)	0.3305(2)	51(3)	Ge(3L)	0.1094(4)	0.2938(7)	0.2340(2)	52(3)
Ge(2I)	0.5113(4)	0.6985(6)	0.3130(2)	48(3)	Ge(4L)*	0.1774(8)	0.182(1)	0.2805(4)	31(3)
Ge(3I)	0.6163(4)	0.8309(6)	0.3258(2)	36(2)	Ge(4L′)*	0.1645(8)	0.143(1)	0.2891(4)	31
Ge(4I)	0.6847(4)	0.7042(6)	0.2866(2)	36(2)	Ge(5L)	0.1329(4)	0.2977(6)	0.3303(2)	44(2)
Ge(5I)	0.5873(4)	0.5742(6)	0.2732(2)	46(3)	Ge(6L)*	0.0152(8)	0.267(1)	0.3196(4)	42(4)
Ge(6I)	0.5108(4)	0.7112(7)	0.2503(2)	51(3)	Ge(6L′)*	0.0267(8)	0.334(1)	0.3220(4)	42
Ge(7I)	0.5272(4)	0.8786(6)	0.2854(2)	45(2)	Ge(7L)	0.0043(4)	0.2841(7)	0.2597(2)	65(3)
Ge(8I)	0.6369(4)	0.8819(7)	0.2674(2)	58(3)	Ge(8L)	0.0699(4)	0.1194(7)	0.2540(2)	51(3)
Ge(9I)	0.6214(4)	0.7169(7)	0.2333(2)	50(3)	Ge(9L)*	0.0867(8)	0.113(1)	0.3151(4)	45(4)
Ge(1J)*	0.511(1)	0.166(1)	0.5245(5)	35(3)	Ge(9L′)*	0.0571(8)	0.149(1)	0.3168(4)	45
Na(1)	0.498(1)	0.078(2)	0.4398(6)	45(8)	Na(25)	0.259(1)	0.195(2)	0.1333(6)	49(8)
Na(2)	0.338(1)	0.907(2)	0.1843(5)	22(7)	Na(26)	0.220(1)	0.437(2)	0.0493(6)	47(8)
Na(3)	0.090(1)	0.307(2)	0.1621(6)	48(8)	Na(27)	0.060(1)	0.701(2)	0.1163(6)	50(8)
Na(4)	0.223(1)	0.720(2)	0.1669(6)	44(8)	Na(28)	0.489(1)	0.032(2)	0.1268(6)	45(8)
Na(5)	0.390(1)	0.789(2)	0.4210(6)	51(9)	Na(29)	0.673(1)	0.982(2)	0.3768(7)	58(9)
Na(6)	0.166(1)	0.600(2)	0.3110(6)	43(8)	Na(30)	0.983(1)	0.482(2)	0.1352(6)	40(8)
Na(7)	0.374(1)	0.691(2)	0.3323(6)	58(9)	Na(31)	0.593(1)	0.380(2)	0.4789(6)	42(8)
Na(8)	0.113(1)	0.233(2)	0.0829(6)	42(8)	Na(32)	0.229(1)	0.787(2)	0.0893(6)	51(9)
Na(9)	0.291(1)	0.300(2)	0.3278(6)	48(8)	Na(33)	0.278(1)	0.023(2)	0.2907(7)	55(9)
Na(10)	0.188(1)	0.918(2)	0.4525(6)	44(8)	Na(34)	0.429(1)	0.258(2)	0.3833(7)	60(9)
Na(11)	0.197(1)	0.091(2)	0.2098(7)	52(9)	Na(35)	0.229(2)	0.451(2)	0.2025(8)	74(11)
Na(12)	0.298(1)	0.196(2)	0.4298(6)	51(8)	Na(36)	0.332(1)	0.950(2)	0.1020(7)	60(9)
Na(13)	0.182(1)	0.433(2)	0.3871(6)	33(7)	Na(37)	0.998(1)	0.106(2)	0.1857(7)	67(10)
Na(14)	0.116(1)	0.870(2)	0.2764(6)	43(8)	Na(38)	0.447(2)	0.440(2)	0.4437(7)	76(11)
Na(15)	0.299(1)	0.525(2)	0.2807(7)	63(10)	Na(39)	0.351(2)	0.969(2)	0.4737(7)	69(10)
Na(16)	0.920(1)	0.144(2)	0.0514(6)	51(9)	Na(40)	0.651(2)	0.154(3)	0.4413(8)	104(13)
Na(17)	0.243(1)	0.703(2)	0.4101(6)	53(9)	Na(41)	0.170(1)	0.081(2)	0.3764(6)	56(9)
Na(18)	0.288(1)	0.511(2)	0.4597(6)	49(8)	Na(42)	0.388(2)	0.850(2)	0.2667(7)	76(10)
Na(19)	0.408(1)	0.619(2)	0.1983(6)	54(9)	Na(43)	0.105(2)	0.889(3)	0.5335(8)	92(12)
Na(20)	0.990(1)	0.404(2)	0.0580(6)	35(8)	Na(44)	0.111(2)	0.873(2)	0.1936(7)	76(10)
Na(21)	0.070(1)	0.569(2)	0.2198(7)	58(9)	Na(45)	0.222(2)	0.831(2)	0.3466(7)	79(11)
Na(22)	0.497(1)	0.906(2)	0.3647(6)	38(8)	Na(46)	0.436(2)	0.098(2)	0.3219(7)	77(10)
Na(23)	0.247(1)	0.101(2)	0.0352(6)	53(9)	Na(47)	0.000(2)	0.987(3)	0.1131(9)	100(13)
Na(24)	0.529(1)	0.925(2)	0.2074(7)	57(9)	Na(48)	0.883(2)	0.071(2)	0.9627(8)	79(11)

Ge_4 case) or 1−9(Ge_9), and Y is the cluster name. In the average model, the names of the Ge_4 units are A, B, C, D, E, F, G and H, and those of the Ge_9 units are I, $\bar{J}$, $\bar{K}$ and $\bar{L}$. In the split model, the Ge_4 clusters remain with the same name and for the Ge_9 clusters Y = I, J, K, L, J′, K′, L′. The pairs (J, J′), (K′, K) and (L, L′) are the 'split' units corresponding to the average $\bar{J}$, $\bar{K}$ and $\bar{L}$ clusters. In all Ge_9 units, except in K′ and L′, the *apica*l atom (Ge_{apic} in the upper-right drawing in Fig. 3) is labelled as Ge(1Y), the four equatorial atoms are those with $i = 2 - 5$ and the four basal atoms are those with $i = 6 - 9$. This kind of description used for a monocapped tetragonal antiprism (ideal form of a 40 electron *nido*-$[Ge_9]^{4-}$ cluster) is called {1,4,4} setting. To have a comparable {1,4,4} setting for the distorted K′ and L′ units, the Ge(7K′) and Ge(6L′) were chosen as *apical* atoms and the equatorial and basal atoms were consequently defined. The *d*(Ge−Ge) distances in the Ge_9 units are sorted into four groups, which are labelled as

Table 3 Important Ge−Ge bond lengths (in Å) for each cluster in $Na_{12}Ge_{17}$. In the list, the Ge(*i*Y) labels are abbreviated as *i*Y (*i* = 1−9; Y = A, B, ..., K′, L′). See also text. The standard deviation for each distance is 0.01 Å except for those concerning split positions (e.s.d. = 0.02−0.03 Å).

Ge$_4$						Ge$_9$																				
1A	−2A	2.59	1E	−2E	2.55	1I	−2I	2.54	1J	−2J	2.56	1K	−2K	2.61	1L	−2L	2.43	1J′	−2J	2.62	7K′	−2K	2.62	6L′	−2L′	2.56
	−3A	2.62		−3E	2.55		−3I	2.53		−3J	2.55		−3K	2.50		−3L	2.65		−3J′	2.62		−3K′	2.52		−5L	2.41
	−4A	2.56		−4E	2.55		−4I	2.57		−4J	2.61		−4K	2.55		−4L	2.49		−4J	2.61		−6K′	2.68		−7L	2.70
2A	−3A	2.56	2E	−3E	2.57		−5I	2.56		−5J	2.57		−5K	2.57		−5L	2.47		−5J′	2.65		−8K′	2.48		−9L′	2.48
	−4A	2.58		−4E	2.54																					
3A	−4A	2.53	3E	−4E	2.52	2I	−3I	2.92	2J	−3J	2.81	2K	−3K	2.76	2L	−3L	2.99	2J	−3J′	3.16	2K	−3K′	3.18	2L′	−5L	2.93
							−5I	2.87		−5J	2.97		−5K	2.92		−5L	2.68		−5J′	2.62		−6K′	2.66		−7L	2.65
1B	−3B	2.54	1F	−2F	2.53	3I	−4I	2.77	3J	−4J	2.81	3K	−4K	2.80	3L	−4L	2.82	3J′	−4J	2.68	3K′	−8K′	2.66	5L	−9L′	2.59
	−2B	2.55		−3F	2.57	4I	−5I	2.77	4J	−5J	2.76	4K	−5K	2.82	4L	−5L	2.75	4J	−5J′	2.88	6K′	−8K′	3.00	7L	−9L′	3.14
	−4B	2.50		−4F	2.55																					
2B	−3B	2.57	2F	−3F	2.57	2I	−6I	2.61	2J	−6J	2.53	2K	−6K	2.55	2L	−6L	2.64	2J	−6J	2.53	1K	−2K	2.61	1L′	−2L′	2.55
	−4B	2.53		−4F	2.54		−7I	2.60		−7J	2.59		−7K	2.41		−7L	2.58		−7J	2.59		−3K′	2.67		−5L	2.65
3B	−4B	2.55	3F	−4F	2.54	3I	−7I	2.63	3J	−7J	2.66	3K	−7K	2.58	3L	−7L	2.58	3J′	−7J	2.55	2K	−5K′	2.48	2L′	−3L	2.56
							−8I	2.56		−8J	2.61		−8K	2.59		−8L	2.54		−8J′	2.57	3K′	−4K	2.55	3L	−7L	2.58
1C	−2C	2.59	1G	−2G	2.51	4I	−8I	2.62	4J	−8J	2.61	4K	−8K	2.60	4L	−8L	2.72	4J	−8J′	2.66	4K	−8K′	2.65	4L′	−5L	2.72
	−3C	2.56		−3G	2.56		−9I	2.60		−9J	2.49		−9K	2.63		−9L	2.65		−9J′	2.53	5K′	−6K′	2.69		−9L′	2.66
	−4C	2.54		−4G	2.54	5I	−6I	2.60	5J	−6J	2.63	5K	−6K	2.54	5L	−6L	2.66	5J′	−6J	2.63	6K′	−9K′	2.68	7L	−8L	2.57
2C	−3C	2.58	2G	−3G	2.57		−9I	2.59		−9J	2.52		−9K	2.59		−9L	2.65		−9J′	2.59	8K′	−9K′	2.67	8L	−9L′	2.66
	−4C	2.57		−4G	2.59																					
3C	−4C	2.57	3G	−4G	2.53	6I	−7I	2.61	6J	−7J	2.59	6K	−7K	2.64	6L	−7L	2.51	6J	−7J	2.59	1K	−4K	2.55	1L′	−3L	2.46
							−9I	2.56		−9J	2.60		−9K	2.54		−9L	2.54		−9J′	2.59		−5K′	2.55		−4L′	2.59
1D	−2D	2.56	1H	−2H	2.52	7I	−8I	2.56	7J	−8J	2.59	7K	−8K	2.70	7L	−8L	2.57	7J	−8J′	2.65	4K	−9K′	2.42	3L	−8L	2.54
	−3D	2.55		−3H	2.52	8I	−9I	2.56	8J	−9J	2.65	8K	−9K	2.58	8L	−9L	2.56	8J′	−9J′	2.54	5K′	−9K′	2.58	4L′	−8L	2.54
	−4D	2.55		−4H	2.55																					
2D	−3D	2.54	2H	−3H	2.53	6I	−8I	3.60	6J	−8J	3.67	6K	−8K	3.70	6L	−8L	3.56	6J	−8J′	3.35	4K	−5K′	3.25	3L	−4L′	3.21
	−4D	2.60		−4H	2.57																					
3D	−4D	2.58	3H	−4H	2.57																					

d_j ($j = 1 - 4$) in the upper-right drawing in Fig. 3 (a fifth type of distance d_5 is also indicated in this figure by a shade line). In Table 3, the distances for the Ge_9 units are listed in the following order: first d_1 (4×) distances (between the apical and the equatorial atoms), then the d_2 (4×) distances (exclusively among equatorial atoms), followed by the d_3 (8×) distances (between equatorial and basal atoms) and the d_4 (4×) distances (exclusively among basal atoms). The shortest d_5 distance is listed at the end of Table 3 (this distance is also indicated in all units in Fig. 3 to help the reader on the comparison).

As illustrated in Figs. 2a and 2b, the eight crystallographically independent types of Ge_4 clusters (A to H) appear more or less as regular tetrahedra. In the average model of the Ge_9 clusters, the cluster I has a regular form and the $\bar{J}$, $\bar{K}$ and $\bar{L}$ units appear clearly distorted. In the split model, 7 kinds of Ge_9 clusters (I, J, K, L, J′, K′, L′) were distinguished. For comparison, in Fig. 3 (short-range ordering models except for I) all Ge_9 clusters were drawn in the {1,4,4} setting of the SAPR-9 polyhedra (monocapped tetragonal antiprism, i.e. a 40 electron *nido*-cluster of $4mm$-C_{4v} symmetry). Compared to an ideal monocapped tetragonal antiprism, the clusters I, J, K and L are only slightly distorted. Roughly, the clusters J′, K′ and L′ appear to have a hybrid form between a SAPR-9 polyhedron and a tricapped trigonal prism (TPRS-9; $\bar{6}m2$-D_{3h}). This form corresponds to a *closo*-$[Ge_9]^{2-}$ cluster (38 electrons), which should have a significant smaller volume than a SAPR-9 *nido*-cluster. However, as reported below, independently of the form of the clusters all of them have practically the same volume, which is an indication that they all belong to the 40 electron system $[Ge_9]^{4-}$.

Applying the analysis used in [14, 15] for the X_9 units (X = Si, Ge, Sn) and neglecting the deviations from $4mm$ symmetry, the seven different Ge_9 cluster anions are characterised by the average bond lengths $\bar{d}_1 = 2.56(4)$ Å, $\bar{d}_2 = 2.83(2)$ Å, $\bar{d}_3 = 2.60(2)$ Å, $\bar{d}_4 = 2.57(3)$ Å and $\bar{d}_5 = \bar{d}_4 \cdot \sqrt{2} = 3.63$ Å. (Fig. 3). In other words, there are only two effective bond lengths, namely $D_1 = 2.58$ Å (from $d_1 \approx d_3 \approx d_4$) and $D_2 = 2.83$ Å (from d_2). From these values, the calculated volume of a Ge_9 polyhedron in $Na_{12}Ge_{17}$ is on average $V_p = 21.99$ Å^3. These data corresponds well with the those of e.g. *Somer* et al. [14] (2.57 Å, 2.84 Å, 21.85 Å^3), *Belin* et al. [16] (2.58 Å, 2.81 Å, 21.88 Å^3) and *Quenéau* and *Sevov* [17] (2.59 Å, 2.83 Å, 22.19 Å^3). In detail, the volumes V_p of the Ge_9 clusters are very similar: 21.80, 22.08, 21.99, 21.50, 22.33, 22.20 and 21.55 Å^3 for the units I, J, K, L, J′, K′ and L′, respectively. For the J′, K′ and L′ clusters equivalent values were obtained when they were assumed to have the form of TPRS-9 polyhedra. The d_1 values for the L, J′, K′ and L′ units vary in the large range of 2.41 to 2.72 Å. The deformation of these units might be the result of the Na−Ge interactions (associated with the type of bridging-ligand function that plays each Na atom).

Each $[Ge_9]^{4-}$ anion has 19 to 20 Na^+ neighbours (the cluster I with Na neighbours is shown in Fig. 2c), and each $[Ge_4]^{4-}$ cluster has 14 to 15 Na^+ neighbours. Each Na atom

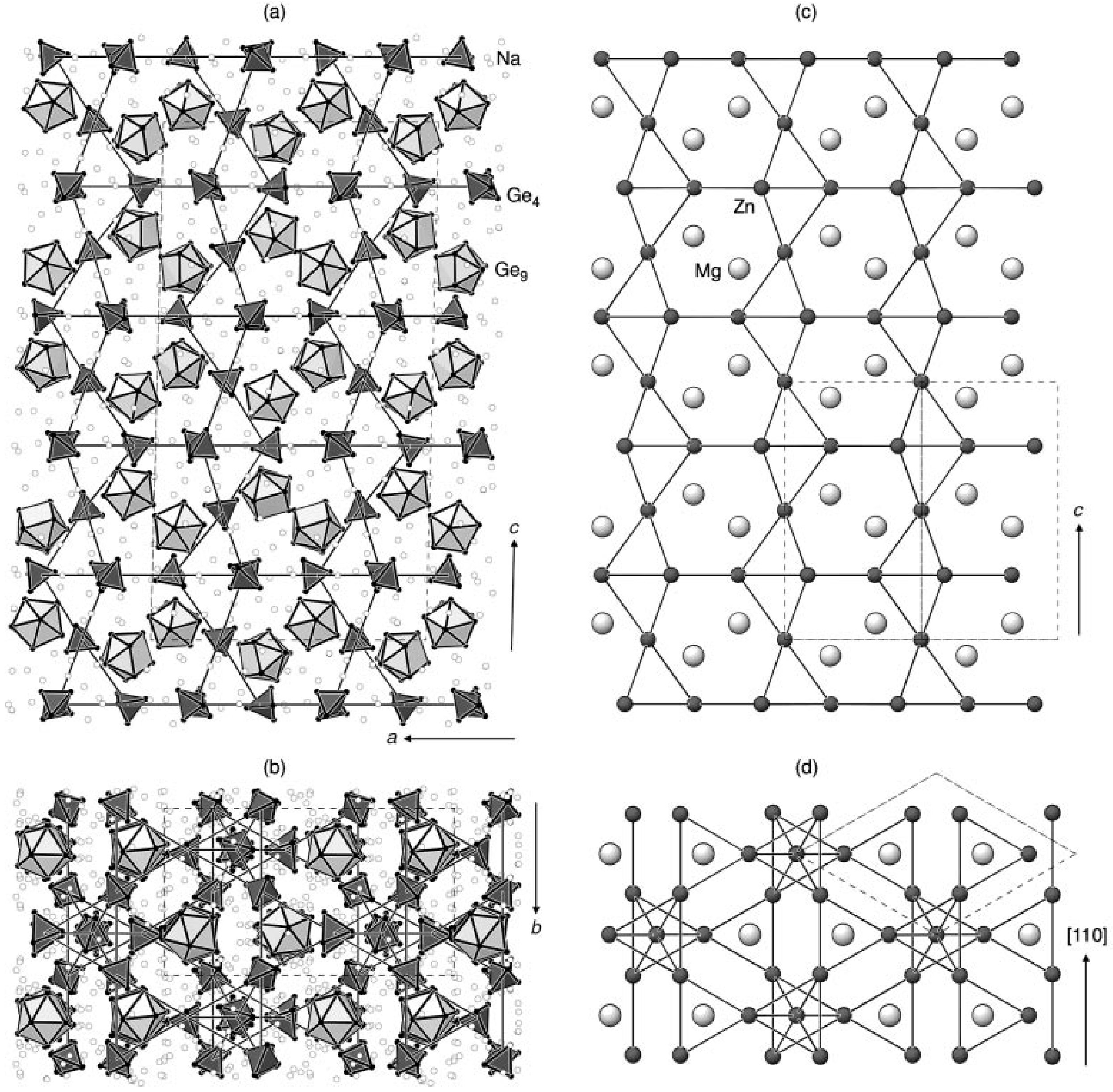

Fig. 1 Projections of the structure of $Na_{12}Ge_{17}$ (a) along the *b* axis and (b) along the *c* axis, and of $MgZn_2$ (c) along [110] and (d) along the hexagonal *c* axis. This demonstrates the relationship between the *basic* structure ($MgZn_2$) and the hierarchical derivative structure ($Na_{12}Ge_{17}$) by atom-by-cluster replacement plus filling 12 of the 17 tetrahedral holes: $\square_{17}[Mg][Zn]_2 \mathrel{\hat{=}} (Na^+)_{12}\square_5[Ge_9^{4-}][Ge_4^{4-}]_2$.

belongs to 4 Ge_n clusters and coordinates 6 to 8 Ge atoms of the neighbouring clusters (d(Na−Ge) distances in the range 2.89 − 3.81 Å) acting as *exo*- and bridging ligands of the μ_2, μ_3, μ_4 type.

Without considering strictly the details of the ordering of X_9 clusters, $Na_{12}Ge_{17}$ is isostructural with $Rb_{12}Si_{17}$ [18]. In the latter structure, however, the splitting of Si sites for the distorted B, C and D type Si_9 clusters was overlooked or could not be observed (Si is a weaker X-ray scatterer than Ge). Also, in the structure refinements of the title compound (Table 1) and $Rb_{12}Si_{17}$ ($R_{gt}(F)$ =0.176 for $I > 2\sigma\cdot(I)$ [18]) the conventional *R*-values are relative large and several alkali metal positions disclose large U_{iso} values, which seems to be mainly a consequence of the incomplete orientational ordering of the X_9 clusters.

As far as we know, there are six $M_{12}X_{17}$ structures ($Na_{12}Ge_{17}$, $Rb_{12}Si_{17}$, $K_{12}Ge_{17}$ [5], $K_{12}Sn_{17}$ [15, 18], $Cs_{12}Sn_{17}$ [15] and the recently discovered $K_{12}Si_{17}$ phase [19]) which belong to the hierarchical cluster replacement $MgZn_2$ family. Only $Rb_{12}Sn_{17}$ belongs to the hierarchical cluster replacement $MgCu_2$ family [20].

3.2 Vibrational Spectrum

The geometrical optimisation for the bare cluster anions $[Ge_9]^{4-}$and $[Pb_9]^{4-}$ [21] by quantum chemical calculations

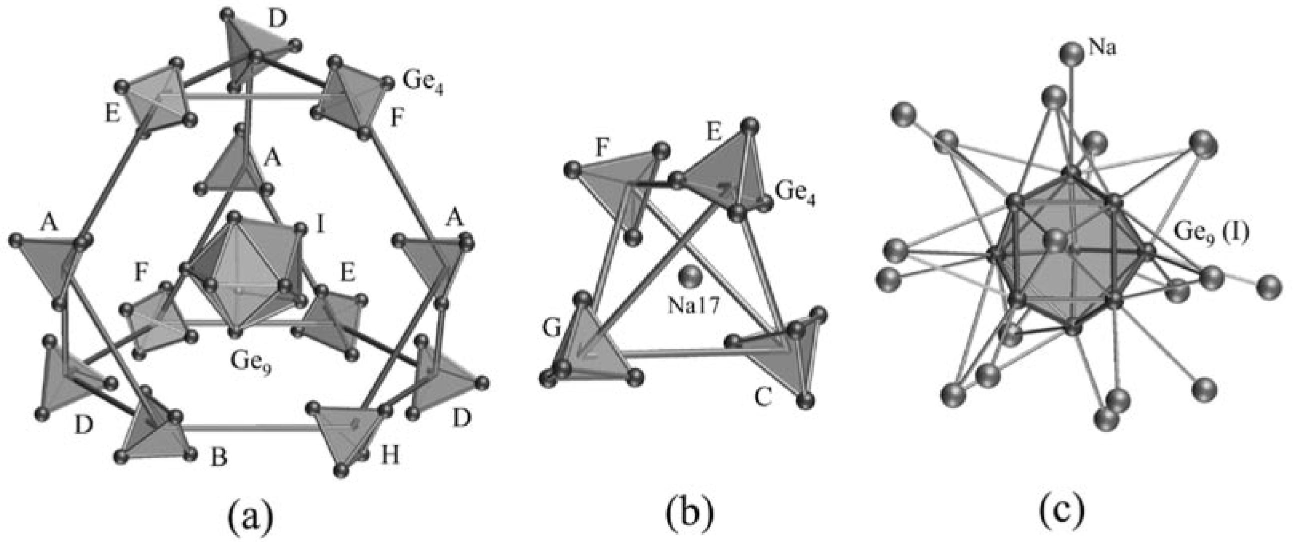

(a) (b) (c)

Fig. 2 Some details of the $Na_{12}Ge_{17}$ structure. (a) A *truncated supertetrahedron* of Ge_4 tetrahedra centred by a Ge_9 unit. (b) A *supertetrahedron* of Ge_4 tetrahedra centred by Na17. (c) A Ge_9 unit of type I with Na neighbours (several of them capping the polyhedron faces). In (a) and (b) the polyhedra are labelled (see text and Tables 2, 3).

have revealed that the SAPR-9 arrangement with the C_{4v}-$4mm$ symmetry is energetically most favoured, however, with only a small energy difference to the other possible configuration TPRS-9. Thus, as stated before, the observed deviations from the C_{4v} symmetry result probably from packing and coordination effects in the crystalline solid state. The calculation of the Raman intensities for the Si_9 and Ge_9 [21] clusters with C_{4v} and D_{3h} symmetries using quantum chemical methods indicate that the SAPR-9 and TPRS-9 clusters are practically indistinguishable in Raman spectra [22]. Therefore, the interpretation of the spectra will be done based on the C_{4v} symmetry of the majority cluster component SAPR-9. However, the coexistence of the different Ge_9 clusters in the solid state is expected to give rise to a broadening of the characteristic Ge_9 bands.

The spectroscopical relevant units in $Na_{12}Ge_{17}$ are the anions $[Ge_4]^{4-}$ and $[Ge_9]^{4-}$ with the idealised symmetry T_d-$\bar{4}3m$ and C_{4v}-$4mm$ (respectively, for which a total of 26 Raman active fundamentals (i.e. 18 bands) are expected:

$[Ge_4]^{4-}$ (T_d-$\bar{4}3m$): $\Gamma_{vib} = A_1\ (R) + E\ (R) + F_2\ (R, IR)$

$[Ge_9]^{4-}$ (C_{4v}-$4mm$): $\Gamma_{vib} = 4A_1\ (R, IR) + A_2\ (-, -) + 3B_1\ (R) + 3B_2\ (R) + 5E\ (R, IR)$.

Instead of the expected eighteen bands, only four broad bands at 274, 222, 207 and 166 cm^{-1} are observed (Fig. 4), two of them (274 and 207 cm^{-1}) represent the four internal modes A_1 and F_2 of the hetero-tetrahedranide anion $[Ge_4]^{4-}$ [23, 24]. Based on the Raman spectrum of Na_4Ge_4 (Fig 5), the remaining E mode is expected to appear as a band of weak intensity around 164 cm^{-1}. Accordingly, the broad and medium strong band at 166 cm^{-1} could represent the missing fundamental E. However, both the shape and the observed intensity indicate an overlap of the E mode with at least one of the Ge_9 fundamentals in this wave region. The most intense band of the spectrum appears at 222 cm^{-1} and is assigned to the breathing mode of the $[Ge_9]^{4-}$ cluster [5, 14]. The Raman spectrum of the $[Ge_9]^{4-}$ anion in the alkali metal compounds M_4Ge_9 (M = K, Rb, Cs) has been investigated quite extensively [5] and exhibits beside the breathing mode at 222 cm^{-1}, two bands of medium intensity at 147 and 164 cm^{-1} and additional two of very weak intensity at 188 and 241 cm^{-1}, respectively. The absence of the remaining 10 Ge_9 bands in the Raman spectrum of $Na_{12}Ge_{17}$ is, as discussed for the $[Ge_9]^{4-}$ cluster in the M_4Ge_9 series [5], mainly due to the accidental coincidences and low intensities. Another reason is the above mentioned overlap of the Ge_9 (147, 164 cm^{-1}) and Ge_4 (164 cm^{-1}) modes in the wave region 140 − 170 cm^{-1} so that only one broad band at 166 $cm^{-1}$is observed instead. Also broad is the characteristic Ge_9 band at 222 cm^{-1}. The broadening effect indicates the coexistence of several Ge_9 species which are slightly different in their spatial arrangements- and hence in their wave numbers-, as found in the X-ray structure study. The Raman spectrum confirms, thus, the presence of two different cluster anions $[Ge_4]^{4-}$ and $[Ge_9]^{4-}$ with very specific intensity patterns and characteristic wavenumbers. The results are in good accordance with those for the compounds $M_{12}Ge_{17}$ (M = K, Rb, Cs) [5] and $M_{12}Sn_{17}$ (M = K, Rb, Cs) [15]. Using the characteristic "cluster breathing" modes at $\nu = 274\ cm^{-1}$ (Ge_4) and $\nu = 222\ cm^{-1}$ (Ge_9) as fingerprints (because these modes are the most intense and do not overlap), one can easily follow *in-situ* the dissolution process that $Na_{12}Ge_{17}$ undergoes in ethylenediamine (*en*) and liquid ammonia. Already in the early 1930's, *Zintl* [25] and *Johnson* [26] had found that the intermetallic binaries $NaGe_x$ and Na_4Ge_x are slightly soluble in liquid NH_3, generating red-brown solutions. Later, *Kummer* and *Corbett* [6, 16] have utilised different sodium and potassium germanides of varying compositions MGe_x ($x = 1.3 -$

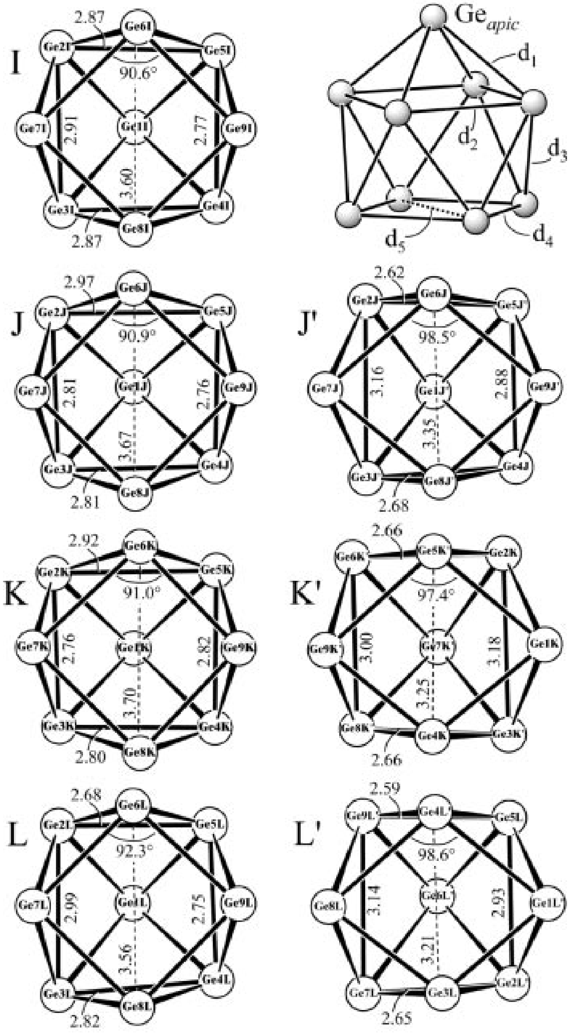

Fig. 3 The seven types of Ge_9 clusters in $Na_{12}Ge_{17}$, as revealed from the split-model structure refinement. In the upper right figure ({1,4,4} setting of a monocapped square antiprism SAPR-9), the distances d_j are defined. For other details see text.

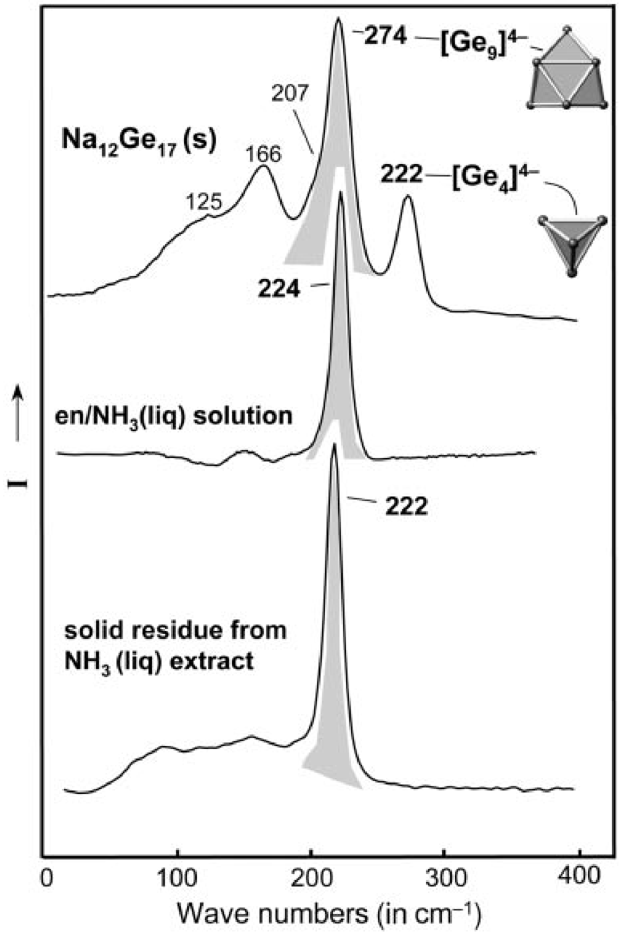

Fig. 4 Raman spectra of $Na_{12}Ge_{17}$, of an extraction by a liquid NH_3/*en* mixture, and of the solid residue left after evaporation of the solvent. Both extracts contain exclusively $[Ge_9]^{4-}$ clusters.

2.25) as precursors for the synthesis of the *en* solvates and cryptates and obtained in all cases brown-green (Na) or red (K) solutions. $Na_{12}Ge_{17}$ is only partially soluble in liquid ammonia and in *en*. The solutions are red and turbid green-brown, respectively. The turbidity of *en* solutions originates probably from a sol-gel process in which micro- and nano-scaled Ge particles are participated and the green-brown coloration seems to be more or less a light scattering effect. Indeed, the use of different mixtures of *en* and liquid ammonia (ratios ≈ 1:1(*en*) − 1:3) results in formation of clear red solutions indicating that such sols are only stable when the solvent ethylenediamine is in large excess or solely present. For the Raman spectroscopic investigations of the solutions, extracts and the residues both *en* and liquid ammonia, as well as their mixtures have been utilised as solvents.

Independent from the nature of the solvent and the colour of the solution, the Raman spectrum of the liquid $Na_{12}Ge_{17}$ extract (cf. Fig. 4) is clearly governed by the very strong and polarised band at 224 cm^{-1} resulting from the cluster anion Ge_9. The evaporation of NH_3 from a liquid ammonia solution yields a dark grey residue which is amorphous to X-rays. The Raman spectrum (Fig. 4) again exhibits the characteristic Ge_9 mode at 222 cm^{-1}. The charge of 4− for the Ge_9 cluster was confirmed by the subsequent elemental analysis yielding a molar ratio Na:Ge = 3.94 : 9. For the characterisation of the insoluble residue from the $Na_{12}Ge_{17}$ extraction, a separate soxhlet experiment with liquid ammonia as solvent has been carried out using ca. 0.5 g of the title compound as starting material and proceeded for 24 h until the dissolution of the Ge_9 component was completed. The dark grey residue obtained after this process shows the Raman spectrum of single phase Na_4Ge_4 (Fig. 5), indicating that the solubility of $Na_{12}Ge_{17}$ is only partially. The soluble constituents are solely Na^+ and $[Ge_9]^{4-}$ leaving the insoluble Na_4Ge_4 in the residue. These findings are in good agreement with previous reports, in which all attempts to dissolve pure Na_4Ge_4 in the respective solvents have failed yet [6].

By heating up, the solvate $Na_4Ge_9(NH_3)_x$ after releasing NH_3(g) decomposes at 742 K into $Na_{12}Ge_{17}$ and Ge as

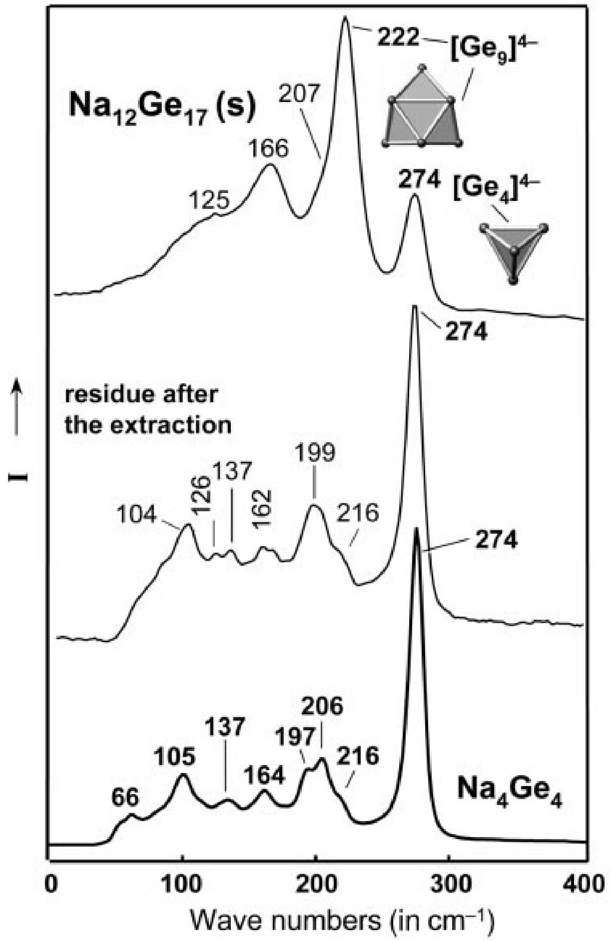

Fig. 5 Raman spectra of $Na_{12}Ge_{17}$ and from its solid residue obtained after the extraction by liquid ammonia, in comparison with that of single phase Na_4Ge_4 (solid).

solid products (Raman spectra and X-rays diffraction results): $3Na_4Ge_9 \rightarrow Na_{12}Ge_{17} + 10Ge$.

4 Experimental

4.1 Syntheses

$Na_{12}Ge_{17}$ was prepared from stoichiometric mixtures of the elements in sealed niobium ampoules or in alumina crucibles sealed in stainless ampoules. The samples were heated up to 1275 K (2h), annealed at 1025 K (48 h) and cooled down to room temperature during 32 h. The metallic grey compound is very sensitive to air and moisture and must be stored and handled under inert conditions (i.e. Glove box; O_2 and H_2O: < 1 ppm).

4.2 X-Ray diffraction measurements

The reflection intensity data were collected with a STOE-IPDS diffractometer (Ag $K\alpha$ radiation) at room temperature. The crystal shape optimisation was performed using X. Shape [9], and the numerical absorption correction was done using the WinGX program package [10]. The structure was solved using SHELXS-97 and refined on F^2 using SHELXL-97. Other details are given in Table 1.

The unit cell parameters (unit cell **I**) of the crystal studied were determined from the least-squares refinement of the 2θ values of 794 reflections ($2° < 2\theta < 29°$).

4.3 Raman spectrum measurements

The FT-Raman spectra of the powdered samples and of the solutions were recorded in sealed pyrex (∅ = 4 mm, thickness = 0.5 mm) and NMR tubes (∅ = 4 mm), respectively, with a the Bruker RFS 100/S spectrometer (Nd: YAG-Laser, 1064 nm, 200 mW).

Acknowledgement. We thank the *Fonds der Chemischen Industrie* for financial support.

References

[1] E. Hohmann, *Z. Anorg. Allg. Chem.* **1948**, *257*, 113.
[2] R. Schäfer, W. Klemm, *Z. Anorg. Allg. Chem.* **1961**, *312*, 214.
[3] J. Witte, H. G. von Schnering, W. Klemm, *Z. Anorg. Allg. Chem.* **1964**, *327*, 260.
[4] F. Potemkin, R. A. Sizov, L. I. Zusman, M. E. Drits, *Izv. AN SSSR. Metally* **1989**, No. 3, 197.
[5] H. G. von Schnering, M. Baitinger, U. Bolle, W. Carrillo-Cabrera, J. Curda, Y. Grin, F. Heinemann, J. Llanos, K. Peters, A. Schmeding, M. Somer, *Z. Anorg. Allg. Chem.* **1997**, *623*, 1037.
[6] L. Diehl, *Dissertation*, Universität Karlsruhe **1971**.
[7] D. Kummer, L. Diehl, *Angew. Chem.*, **1970**, *82*, 881; *Angew. Chem. Int. Engl.* **1970**, *9*, 895
[8] J. Llanos, *Dissertation*, Univ. Stuttgart, **1984**.
[9] X. Shape 1.03, Crystal Optimization for Numerical Absorption Correction, Stoe & Cie GmbH, Darmstadt, Germany, **1998**.
[10] L. J. Farrugia, WinGX, *J. Appl. Crystallogr.* **1999**, *32*, 837.
[11] G. M. Sheldrick, SHELXS-97, Programs for the Solution of Crystal Structures, University of Göttingen **1997**.
[12] G. M. Sheldrick, SHELXL-97, Programs for Crystal Structure determinations, University of Göttingen **1997**.
[13] W. Carrillo-Cabrera, N. Caroca-Canales, H. G. von Schnering, *Z. Anorg. Allg. Chem.* **1994**, *620*, 247.
[14] M. Somer, W. Carrillo-Cabrera, E. M. Peters, K. Peters and H. G. von Schnering, *Z. Anorg. Allg. Chem.* **1998,** *624*, 1915.
[15] M. Baitinger, *Dissertation*, Tech. Univ. Darmstadt, **2000**.
[16] C. H. E. Belin, J. D. Corbett, A. Cisar, *J. Am. Chem. Soc.* **1977**, *99*, 7163.
[17] V. Queneau, S. C. Sevov, *Angew. Chem.* **1997** *109*, 1818; *Angew. Chem. Int. Ed. Engl.* **1997**, *36*, 1754.
[18] V. Queneau, E. Todorov, S. C. Sevov, *J. Am. Chem. Soc.* **1998**, *120*, 3263.
[19] C. Hoch, M. Wendorff, C. Röhr, *Z. Anorg. Allg. Chem.* **2002**, *628*, 2172.
[20] C. Hoch, P. Zönnchen, C. Röhr, *Twentieth European Crystallographic Meeting*, Prag, Vol. 5, **1998**, 388.
[21] H. G. von Schnering, M. Somer, M. Kaupp, W. Carrillo-Cabrera, M. Baitinger, A. Schmeding, Y. Grin, *Angew. Chem.* **1998** *110*, 2507; *Angew. Chem. Int. Ed.* **1998**, *37*, 2359.
[22] M. Kaupp, *private communication*.
[23] G. Kliche, H. G. von Schnering, *Z. Anorg. Allg. Chem.* **1992**, *608*, 131.
[24] M. Somer, *Z. Anorg. Allg. Chem.* **2000**, *626*, 2478.
[25] E. Zintl. H. Kaiser, *Z. Anorg. Allg. Chem.* **1934**, *216*, 273.
[26] W. C. Johnson, A. C. Wheatley, *Z. Anorg. Allg. Chem.* **1933**, *211*, 113.